

Diamagnetism and flux creep in bilayer exciton superfluids

P. R. Eastham,¹ N. R. Cooper,² and D. K. K. Lee³

¹School of Physics, Trinity College, Dublin 2, Ireland.

²T.C.M. Group, Cavendish Laboratory, J.J. Thomson Avenue, Cambridge CB3 0HE, United Kingdom

³Blackett Laboratory, Imperial College London, London SW7 2AZ, United Kingdom

(Dated: April 24, 2012)

We discuss the diamagnetism induced in an isolated quantum Hall bilayer with total filling factor $\nu_T = 1$ by an in-plane magnetic field. This is a signature of counterflow superfluidity in these systems. We calculate magnetically induced currents in the presence of pinned vortices nucleated by charge disorder, and predict a history-dependent diamagnetism that could persist on laboratory timescales. For current samples we find that the maximum in-plane moment is small, but with stronger tunneling the moments would be measurable using torque magnetometry. Such experiments would allow the persistent currents of a counterflow superfluid to be observed in an electrically isolated bilayer.

PACS numbers: 73.43.Nq, 73.43.Jn, 73.43.Lp

I. INTRODUCTION

Superfluidity¹ is a spectacular form of hydrodynamics involving dissipationless flow, metastable circulation, and quantization of circulation. It occurs in liquid helium and cold atomic gases, where it is associated with the condensation of many bosons into a single quantum state. Whether condensates of quasiparticles, such as excitons, would also be superfluids has been discussed for many years, with debate over the physical manifestations^{2–8} of superfluid hydrodynamics for quasiparticles, the (related) role of symmetry-breaking perturbations, and the significance of interactions and thermal equilibrium⁹.

This question can now be addressed experimentally, with emerging evidence for the condensation of quasiparticles including excitons, polaritons, and magnons. A particularly interesting system is the quantum Hall bilayer at total filling factor $\nu_T = 1$ (see Fig. 1). This consists of two closely spaced quantum wells, each containing a two-dimensional electron gas, subjected to a strong perpendicular field B_\perp so that the lowest Landau level in each layer is half-filled. The tunneling between the two layers is weak compared to the Coulomb energy scale. When the interlayer separation d is of the order of the magnetic length $l_B = (\hbar/eB_\perp)^{1/2}$, the ground state is believed to be a Bose-Einstein condensate of interlayer excitons^{10–15} caused by the Coulomb attraction of electrons and holes across the layers. (Note that the holes are unfilled electron states of the lowest Landau level of the conduction band.) Flows of these condensed excitons correspond to dissipationless counterflowing electrical currents in the two layers¹². Initial evidence of dissipationless transport came from interlayer tunneling,^{16,17} which exhibits non-zero interlayer currents at negligible interlayer voltages^{12,18–20}. This regime persists up to a critical current, above which dissipation increases rapidly.

The interpretation of transport measurements as evidence²¹ for exciton superfluidity is complicated by parallel charge transport channels, the injection and removal of electrons^{7,22,23} at the contacts, as well as pos-

sible dissipation in the leads. Here, we show that magnetometry on *isolated* bilayers could provide direct evidence for exciton superfluidity, without the complications inherent in transport studies. We predict that, at low temperatures, the bilayer shows a history-dependent susceptibility. Changes in the in-plane field lead to a persistent diamagnetic moment that is, however, not induced by fields present when the condensate forms. This discrepancy corresponds to that between the moments of inertia of normal and superfluid helium inferred in a torsional oscillator experiment.

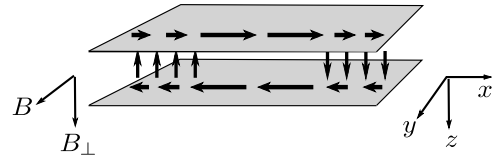


FIG. 1. Schematic diagram of a bilayer of electrons in the quantum Hall regime due to a strong perpendicular field B_\perp . Applying a weak in-plane field B causes counterflowing charge currents as a diamagnetic response. For an isolated bilayer the current loop closes at the edges of the sample by interlayer tunneling. In an excitonic picture, this corresponds to the flow of neutral excitons along the bilayer with recombination at the edges.

The in-plane magnetic susceptibility of the exciton condensate has previously been considered^{6,24–26} in clean bilayers. However, there are very good reasons to expect^{27–30} that disorder is essential for understanding the observed transport properties of the bilayer at low temperatures. In particular, for quantum Hall bilayers, charge disorder nucleates vortices in the condensate^{29–33}. Therefore, we will study in this work the magnetic properties of a quantum Hall bilayer with disorder-induced vortices. We first consider the zero-temperature limit, and show how dissipationless supercurrents lead to long-lived diamagnetic moments. In current samples, the resulting moments are small [Eq. (16)], but for samples with stronger tunneling the moments can be compara-

ble to the Landau diamagnetism. We also consider the effects of non-zero temperatures, and estimate the dissipation due to thermal creep³⁴ of the in-plane flux. This dissipative mechanism gives rise to a non-vanishing resistance for the counterflow supercurrents, and causes the diamagnetic moments to decay in time. Based on the parameters of current experiments, we expect dissipation to be significant, which is consistent with experimental resistance measurements. The flux motion in this regime can be studied in transport experiments. Samples deeper in the condensed phase, however, would show persistent counterflow supercurrents on laboratory timescales, whose presence and eventual decay could be observed by magnetometry.

The remainder of this paper is structured as follows. In Sec. II, we outline the model we consider for the behavior of long-wavelength counterflow supercurrents in the disordered bilayer. In Sec. III, we apply this model to calculate the in-plane susceptibility of the bilayer in the zero-temperature limit. In Sec. IV, we discuss the extension to finite but low temperatures. Finally, in Secs. V and VI, we present numerical estimates for the moments and resistance in experiments, and summarize our conclusions.

II. MODEL AND BACKGROUND

In this work, we consider a quantum Hall bilayer at total filling factor $\nu_T = 1$, in the presence of the disordered electrostatic potential originating from the dopants, set back at a distance d_d . For definiteness, we adopt the “coherence network” picture of Fertig and Murthy,³⁰ although our theory here is more general. In this picture, the random Coulomb field from the dopants creates puddles of normal electron liquid surrounded by channels of excitonic superfluid. In quantum Hall ferromagnets, physical and topological charge are related so that the charge puddles nucleate vortices, known as merons, in the superfluid channels^{29–33}. We estimated³¹ that typical disorder strengths induce on the order of one unpaired vortex per puddle so that the correlation length of this disorder is $\xi \approx d_d \approx 100$ nm.

The energy associated with the excitonic supercurrents in the channels is, in terms of a superfluid phase η ,²⁸

$$H_{\text{eff}} = \int \left[\frac{\rho_s}{2} |\nabla \eta + \mathbf{q}|^2 - t \cos(\eta + \theta_0) \right] d^2r, \quad (1)$$

where the first term is the kinetic energy of the counterflow supercurrent with superfluid stiffness ρ_s , and the second term is the energy of the interlayer tunneling currents with tunneling strength t . The merons introduced by the charge disorder give rise to the random field θ_0 . For the coherence network, both ρ_s and t should be renormalized by the area fraction of the superfluid channels.

Eq. (1) is written in a gauge where the vector potential of the in-plane field B is zero perpendicular to the layers

and non-zero parallel to the layers. This field then appears in the kinetic energy, inducing a wavevector^{6,12,35}

$$\mathbf{q} = (\mathbf{B} \times \hat{\mathbf{z}})ed/\hbar, \quad (2)$$

where d is the interlayer separation. The counterflow and tunneling currents are seen to be

$$\mathbf{j}_{\text{cf}} = \frac{e\rho_s}{\hbar} (\nabla \eta + \mathbf{q}) = \mathbf{j}_{\text{p}} + \mathbf{j}_{\text{d}}, \quad (3)$$

$$j_t = \frac{et}{\hbar} \sin(\eta + \theta_0), \quad (4)$$

so the magnetic field induces a diamagnetic contribution $\mathbf{j}_{\text{d}} = e\rho_s \mathbf{q}/\hbar$ to the counterflow supercurrent \mathbf{j}_{cf} , but does not appear explicitly in the coherent tunneling current j_t . We can make a gauge transformation so that the vector potential is non-zero only perpendicular to the bilayer, in which case the phase transforms to $\eta \rightarrow \eta + \mathbf{q} \cdot \mathbf{r} \equiv \theta$:

$$H_{\text{eff}} = \int \left[\frac{\rho_s}{2} |\nabla \theta|^2 - t \cos(\theta - \mathbf{q} \cdot \mathbf{r} + \theta_0) \right] d^2r. \quad (5)$$

This form for the energy functional highlights the fact that the in-plane magnetic response of the bilayer vanishes if there are no current loops that encircle the field — the field disappears from Eq. (5) when $t = 0$. (A non-zero diamagnetic susceptibility remains possible in multiply-connected geometries³⁵ or at non-zero frequency⁶. We comment on the extension of our results to the Corbino disk geometry in Sec. V.)

At zero temperature, the state of the bilayer is determined by minimizing Eq. (1), which gives

$$-\lambda_J^2 \nabla^2 \eta + \sin(\eta + \theta_0) = 0, \quad \lambda_J = (\rho_s/t)^{1/2}. \quad (6)$$

When $\theta_0 = 0$ this is the pendulum equation, containing the Josephson length λ_J : the characteristic lengthscale over which excitonic supercurrents decay by interlayer tunneling. This scale is estimated to be on the order of a few microns in experiments. We will discuss below the decay of excitonic supercurrents by tunneling in the disordered case, which involves a different lengthscale.

It is useful to recall, for comparison with our treatment of the disordered case, the response^{24,25,36–38} of the clean model ($\theta_0 = 0$) to an in-plane field. For small fields, the ground state will minimize the tunneling energy, and so $\theta \approx \mathbf{q} \cdot \mathbf{r}$ or $\eta \approx 0$. This is the commensurate state, in which the field induces a long-wavelength counterflow supercurrent $\mathbf{j}_{\text{cf}} \approx \mathbf{j}_{\text{d}}$, as in Eq. (3). Thus there is an in-plane magnetic moment of $M_{\parallel} = j_d d L_x L_y = d L_x L_y \chi_0 B / \mu_0$, with the susceptibility

$$\chi_0 = \mu_0 j_d / B = \mu_0 e^2 \rho_s d / \hbar^2. \quad (7)$$

We see that the diamagnetic moment $M_{\parallel} = \chi_0 B$ increases linearly with the in-plane field B in the commensurate state.

In an isolated bilayer, the counterflow currents must vanish at the ends of the sample. This occurs in the commensurate phase because, as dictated by Eq. (6),

the diamagnetic currents in the bulk of the sample are eliminated by tunneling over a region of size λ_J near the sample boundaries (Fig. 1). However, since the phase η is a periodic variable the maximum current which can recombine in this way is given by $e\rho_s|\nabla\eta|/\hbar \sim e\rho_s/\hbar\lambda_J$. If the diamagnetic current present in the bulk exceeds this value, then a net winding of the phase η , in the form of Josephson vortices, enters from the boundaries. This occurs at the field

$$B_0 \sim \hbar/e d \lambda_J. \quad (8)$$

Above B_0 the system is in the incommensurate phase in which the kinetic energy of the counterflow supercurrents dominates so that $\theta \approx 0$ or $\eta \approx -\mathbf{q} \cdot \mathbf{r}$. The net winding in η along the sample implies that the counterflow supercurrents have weak oscillations around zero along the sample, and the diamagnetic moment is small. The field B_0 marks the field above which the diamagnetic susceptibility rapidly decreases from χ_0 as Josephson vortices fill the system and compensate the diamagnetic contribution in Eq. (3).

While in the clean limit the phase twists nucleated at the boundary propagate into the bulk, in the disordered case any such phase twists can be pinned by the disorder. They can thus be kept out of the bulk of the sample, which can continue to contribute the full diamagnetic susceptibility χ_0 . To describe this effect quantitatively we shall use the collective pinning theory we have previously applied^{27,28} to the transport experiments in zero field ($q = 0$).

The starting point for understanding the transport experiments is to note that Eq. (1) is a random-field XY model. The energy H_{eff} consists of the competition between the tunneling energy, which is minimized by a spatially varying superfluid phase η over the disorder correlation length ξ , and the superfluid stiffness, which is minimized by a uniform superfluid phase. For the bilayer, the disorder correlation length is much shorter than the clean tunneling length: $\xi \ll \lambda_J$. In this regime, the superfluid stiffness dominates at short scales, up to the Imry-Ma or pinning length

$$L_d \sim \lambda_J^2/\xi = \rho_s/t\xi \quad (9)$$

where the two energies balance. We estimate²⁸ that $L_d \approx 10 - 100 \mu\text{m}$ and $\rho_s \approx 20 - 100 \text{ mK}$ in experiments. Beyond this scale, the phase rotates to take advantage of the tunneling energy. Therefore, we can interpret the ground state as consisting of randomly polarized domains of size L_d . The total tunneling current in each domain is zero in the ground state because the random field θ_0 gives a current density j_t [Eq. (4)] of random sign within each domain of constant η .

However, if we drive the system by injecting currents phase twists enter from the contacts, leading to configurations with non-zero tunneling currents. Injected counterflow current decays into the bulk *via* tunneling, *i.e.*, recombination of excitons. This tunneling current is sup-

plied by rotating the phase of the domains near the contacts, leaving domains in the bulk in their ground state. The maximum coherent tunneling current that can be supported by each domain is given by²⁸:

$$I_d = e\rho_s/\hbar. \quad (10)$$

If all the domains near the contact are rotated to supply this maximum tunneling, then we see a uniform tunneling current j_t until all the injected counterflow current has decayed by tunneling. Then both the tunneling and counterflow currents are zero in the bulk. This can be described by the continuity equation for the current:

$$L_d^2 \nabla \cdot \mathbf{j}_{\text{cf}} = \pm I_d. \quad (11)$$

where L_d^2 is the size of the domain and I_d is the tunneling current across the layers in the domain. The sign of I_d is determined by what is necessary to reduce the counterflow current. In a one-dimensional geometry, this gives a counterflow current profile that decays linearly into the bulk from the edge. For instance, for an injected current of $-j_i$ at $x = 0$, the current profile in the x -direction is

$$j_{\text{cf}}(x) = \begin{cases} -j_i + I_d x/L_d^2 & 0 < x < x_0 \\ 0 & x > x_0. \end{cases} \quad (12)$$

where the point $x_0 = j_i L_d^2/I_d$ marks the boundary of the region from the sample edge where coherent tunneling occurs to reduce the counterflow current. This current profile is a critical state similar to the Bean critical state in superconductors³⁹. In this state, there is a region near the contact over which the density gradient in the soliton train (introduced by the injected current) balances the pinning force arising from the tunneling.

III. SUSCEPTIBILITY WITH DISORDER: ZERO-TEMPERATURE LIMIT

We now consider the response of the disordered system to an in-plane field at zero temperature. We will see that the disordered system has a different diamagnetic response from the clean system. It does not have a commensurate-incommensurate transition controlled by an intrinsic lengthscale λ_J [see Eq. (8)]. Instead, we find a saturation phenomenon for the diamagnetic moment at a field B_c [see Eq. (15)] controlled by the properties [Eq. (9) and (10)] of the phase-polarized domains, *i.e.*, the disorder-pinning of the applied flux. This is followed by a depinning of the polarized domains and a strong suppression of the diamagnetic response at a higher field $B_{c2} > B_0$ [Eq. (17)] controlled by the disorder correlation length ξ . Such behavior is similar to that of the mixed-state of a superconductor, but very different from that previously predicted for exciton condensates.

We require the response of the superfluid phase η to an in-plane field B , corresponding to a non-zero \mathbf{q} in Eq. (1). To obtain this, we note that Eq. (6) for the phase η does

not depend on the in-plane field. Alternatively, we can see that the superfluid phase is coupled to the field in Eq. (1) as an integral over $\mathbf{q} \cdot \nabla \eta$, which can be written as a boundary term for η . Thus the current distribution in a field can be related to that in zero field with shifted boundary conditions. This observation allows us to apply the critical-state model^{27,28} in zero field, as reviewed above, to calculate the current profile in non-zero field.

For definiteness, we consider a rectangular sample with dimensions L_x and L_y , with the in-plane field in the y -direction. Thus, counterflow currents $\mathbf{j}_{\text{cf}}(x)$ flow in the x -direction, and tunneling currents $j_t(x)$ in the z -direction (see Fig. 1). For an isolated bilayer, $\mathbf{j}_{\text{cf}}(x) = 0$ at $x = 0$ and L_x . We can decompose \mathbf{j}_{cf} into paramagnetic and diamagnetic parts as in Eq. (3). The paramagnetic part, $\mathbf{j}_p = e\rho_s \nabla \eta / \hbar$, obeys the boundary condition $\mathbf{j}_p \cdot \hat{\mathbf{x}}|_{x=0} = \mathbf{j}_p \cdot \hat{\mathbf{x}}|_{x=L_x} = -j_d$. Since the phase η obeys the same equation, Eq. (6), in the bulk irrespective of an in-plane field, \mathbf{j}_p has the same profile as in a system in zero field (when $\mathbf{j}_{\text{cf}} = \mathbf{j}_p$) with a current of $-j_d$ flowing across the boundaries. The full counterflow current \mathbf{j}_{cf} for the isolated bilayer in a field is recovered simply by adding a uniform $+j_d$ to this zero-field profile of $j_p(x)$.

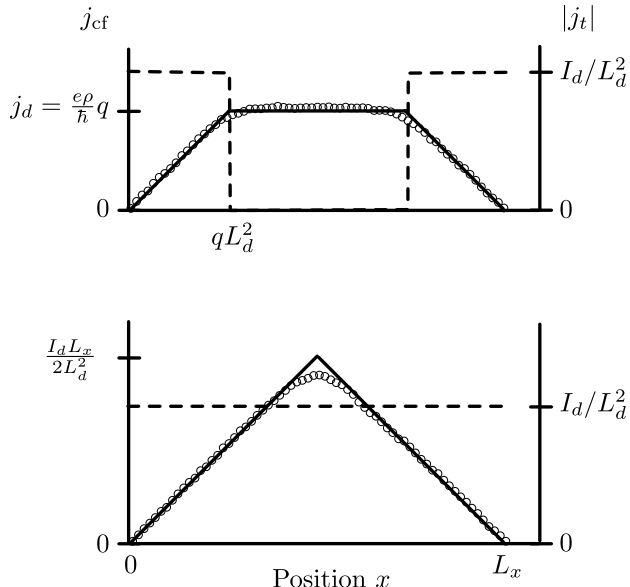


FIG. 2. Profiles of the counterflow (solid lines and circles, left axis) and tunneling (dashed, right axis) currents induced by applying an in-plane field B to a rectangular bilayer (Fig. 1), at zero temperature. The lines show results from the critical-state model, and the circles show numerical results from the microscopic Eq. (6). The top (bottom) panel shows the profile below (above) the critical field B_c [Eq. (14)]. The tunneling currents have opposite signs in the two halves of the sample (not shown). The simulation (circles) is a 200-site lattice model in one dimension with $ta^2/\rho_s = 0.4$, where a is the lattice spacing and $qa = 6$ (top) and 12 (bottom). The disorder is uncorrelated from site to site ($\xi \approx a$).

In the critical-state model as discussed above, the counterflow currents obey Eq. (11) and so $j_p(x)$ decays

linearly in space from $-j_d$ at the edge to zero. In other words, the profile of the paramagnetic current $j_p(x)$ near the $x = 0$ edge is given by Eq. (12) with $j_i = j_d$. The distance x_0 which gives the width of the region where coherent tunneling occurs is determined by the distance where the total counterflow current vanishes: $j_p(x_0) + j_d = 0$. This criterion gives a distance of

$$x_0 = j_d L_d^2 / I_d = q L_d^2 \quad (13)$$

from the edge of the sample. The total current profile is shown in Fig. 2 (top). The figure also shows the tunneling current density $|j_t| = I_d / L_d^2$ which is at its maximal value up to the edge of the tunneling region at qL_d^2 from (either) edge of the sample. Beyond x_0 , there is no paramagnetic contribution to the counterflow current.

This current profile is similar to the one depicted in Fig. 1. A diamagnetic counterflow is generated by the in-plane field in the bulk of the bilayer. However, an isolated bilayer must have zero counterflow current at the edges. In our critical-state model, this is achieved by coherent tunneling *via* phase-polarized domains. The width of this tunneling region is determined by the size of the domain L_d and the coherent tunneling current that each could support I_d . We see that a stronger field gives a higher diamagnetic current and so more domains must be involved. In other words, the size of the tunneling region increases with the in-plane field, as can be seen from Eq. (13): $x_0 \propto q \propto B$. This should be contrasted with the decay length λ_J for the commensurate state of the clean model which is an intrinsic scale that does not vary with the field.

As the parallel field B is increased, the diamagnetic current in the bulk increases linearly with B . This requires a wider tunneling region so that all the current can decay to zero at the edge. So, the tunneling region increasingly penetrates the bulk. This penetration is complete when the width of the region, qL_d^2 , reaches $L_x/2$. This saturation occurs when the field reaches a critical field of

$$B_c = (\hbar/2e)(L_x/dL_d^2) = (\hbar/2e)(L_x \xi^2 t^2 / d\rho_s^2). \quad (14)$$

Beyond this critical field, all the phase domains in the sample take part in coherent tunneling with a constant magnitude for the tunneling current density j_t , as depicted in Fig. 2 (bottom). The counterflow current, therefore, rises linearly from zero from either edge, reaching a maximum at the center of the sample. This saturated current profile stays the same for fields higher than B_c . Note that, whereas the critical field B_0 in the clean limit is a microscopic parameter independent of sample geometry, B_c is proportional to the length of the sample in a disordered system.

We have tested the critical-state model by comparing it with numerical minimization of the energy [Eq. (1)] for a one-dimensional lattice model. To do this we add a dissipative dynamical term $-\dot{\eta}$ to the right-hand side of Eq. (6) and numerically find the resulting steady-state. We begin by finding the steady-state with the

boundary condition $d\eta/dx = 0|_{x=0,L_x}$, corresponding to an isolated bilayer in the absence of an in-plane field. We then slowly increase the boundary condition so that $d\eta/dx|_{x=0,L_x} = -q$, corresponding to applying the in-plane field. The counterflow supercurrent is then obtained from the resulting phase profile by adding the diamagnetic term, as described above. The resulting current profiles, averaged over disorder realizations, are shown as the circles in Fig. 2, and are seen to agree closely with the critical-state model.

We will now discuss the magnetic moment generated by the diamagnetic response of the bilayer. Integrating the current profile gives the moment M_{\parallel} :

$$\frac{\mu_0 M_{\parallel}}{L_x L_y d} = \begin{cases} \chi_0 B \left(1 - \frac{B}{2B_c}\right) & B < B_c \\ \chi_0 B_c / 2 & B \geq B_c. \end{cases} \quad (15)$$

We see that the moment no longer rises linearly with B with the full diamagnetic susceptibility χ_0 of the clean system. This is because, as seen in Fig. 2, the fraction of the sample with the full diamagnetic current j_d is continuously reduced as B (and hence q) increases. In fact, the total moment saturates at the critical field B_c to the value of

$$M_{\parallel,\max} = \frac{e\rho_s L_x}{4\hbar L_d^2} L_x L_y d. \quad (16)$$

The analysis above applies if the field and supercurrents are sufficiently small that their presence does not modify the pinning length L_d , *i.e.*, the supercurrents do not depin the vortices. This is the case if $q < 1/\xi$, the inverse disorder correlation length, so that the additional phase winding at wavevector q in Eq. (5) does not affect the tunneling energy. For larger fields however, the tunnel currents will oscillate within each correlation area, rapidly suppressing the net tunneling at larger scales. The current j_p , which is j_d at the boundary, will then be approximately uniform, and j_{cf} and j_t will be small at long wavelengths. Thus we expect the susceptibility to fall quickly for fields beyond

$$B_{c2} \sim \frac{\hbar}{ed\xi} \sim 0.5\text{T}. \quad (17)$$

This can be regarded as a depinning field where the phase is no longer pinned by the random field but is determined by the diamagnetic wavevector q . A corresponding suppression²⁸ of the current in interlayer tunneling experiments is expected, and observed, at such fields. Since $B_c/B_{c2} = L_x \xi / 2L_d^2 < 1$ for experimental samples with $L_x \sim 1$ mm, the saturation at B_c occurs before this suppression at B_{c2} . Note that in the lattice model discussed above, the disorder is uncorrelated between sites, so that the numerical simulations do not capture the depinning effect at B_{c2} .

IV. FLUX CREEP AND DISSIPATION AT LOW TEMPERATURES

Let us now consider thermal fluctuations over the energy barriers which pin the winding of the superfluid phase. This allows the supercurrents to relax to the equilibrium state with $j_{cf} = 0$ and $j_t = 0$. The diamagnetic moments induced by an in-plane field will decay as phase slips enter the system. This gives rise to resistivity in transport measurements⁴⁰. We will estimate the size of these effects, applying the conventional flux-creep model of superconductors³⁴. We neglect the possibility of vortex-glass states⁴¹, which may further suppress the dissipation at low temperatures.

For sufficiently low temperatures T , the dynamics of the merons controlling the diamagnetic moment will involve thermal fluctuations of the phase domains of size L_d discussed above. As in the Anderson-Kim theory³⁴, uncorrelated vortex motion should be irrelevant at low temperatures and small bias, because the vortex separation $\xi \ll L_d$, so the energy barriers are larger. A thermal fluctuation in which the phase of a domain changes by approximately 2π corresponds to a phase slip moving a distance L_d . This will occur at a frequency $\omega_0 e^{-U(j)/kT}$, where ω_0 is an attempt frequency and $U(j)$ is an energy barrier. Such phase slip dynamics implies an interlayer voltage according to the Josephson relation $V = \hbar\theta/e$. For a typical domain size of L_d , this gives a layer-antisymmetric in-plane electric field

$$E = E_{\text{top}} - E_{\text{bottom}} \approx \frac{\hbar\omega_0}{eL_d} e^{-U(j)/kT}. \quad (18)$$

At zero current, the typical energy barrier $U(j)$ will be the energy of a domain, which is the stiffness ρ_s irrespective of size²⁸ in two dimensions. The barrier will vanish at the current scale associated with the domain, $j_c = I_d/L_d \approx e\rho_s/(\hbar L_d)$. The linear interpolation, $U(j) = \rho_s(1 - j/j_c)$, corresponds to the Anderson-Kim model. Inserting this form in Eq. (18), we obtain for the ohmic regime a sheet resistance for counterflow currents of

$$R_s \approx (\hbar^2 \omega_0 / e^2 kT) e^{-\rho_s/kT}. \quad (kT \ll \rho_s) \quad (19)$$

The in-plane magnetic moment, and the long-wavelength counterflow supercurrent, relaxes in time t as⁴²

$$M_{\parallel}(t)/M_{\parallel,T=0} \approx 1 - (kT/\rho_s) \ln(\omega_0 t), \quad (20)$$

where $M_{\parallel,T=0}$ is the $T = 0$ moment from Eq. (15).

It is possible to extend this argument into the dissipative regime at high bias or temperature, where the barriers become irrelevant. The simplest assumption would be that the domain rotates every attempt time $1/\omega_0$ when the current density is j_c . This gives a resistivity in the flux-flow regime of

$$R_s^* \approx \frac{\hbar^2 \omega_0}{e^2 \rho_s}, \quad (21)$$

so that we can rewrite the flux-creep form as

$$R_s \approx R_s^* e^{-\rho_s/kT}. \quad (22)$$

However, details of the dissipation are likely to change between these two regimes and other parameters may enter R_s^* , so that the prefactor in Eq. (22) will not be exactly the resistivity in the dissipative regime. Provided that R_s^* is not fitted too far from the flux-creep regime, this is unimportant in practice because the exponential factor in general dominates in Eq. (22). Over a wider range of temperatures and currents, effects such as the activation of quasiparticles may appear, leading to additional exponential factors in the dissipation.

Reliable calculations of ω_0 are very difficult, and irrelevant in practice in the flux-creep form, Eq. (22). Nonetheless, an estimate may be obtained by considering the dynamical equation for the phase,^{12,29}

$$\nabla^2 \eta - \frac{1}{\lambda_J^2} \sin(\eta + \theta_0) = \frac{\hbar^2}{e^2 \rho_s} \left[c \ddot{\eta} - \frac{1}{\rho_z} \dot{\eta} - \frac{1}{\rho_{xx}} \nabla^2 \dot{\eta} \right] \quad (23)$$

where ρ_{xx} (ρ_z) is the resistivity of in-plane (tunneling) quasiparticle currents, and c is the interlayer capacitance per unit area. This gives several candidates for the frequency scale at length scale L_d . Since the resistivities are activated, we expect the first (inertial) term in Eq. (23) to control the dynamics at sufficiently low temperatures: $\omega_0 = (e/\hbar L_d)(\rho_s/c)^{1/2}$.

V. DISCUSSION

We have examined the diamagnetic response of an isolated bilayer due to counterflow superfluidity. We obtained an in-plane diamagnetic moment which saturates at a critical value B_c . Our theory also predicts a field scale B_{c2} for the suppression of the in-plane diamagnetic response. There would be no in-plane susceptibility in a field-cooled bilayer, even below B_{c2} , allowing a separation of the superfluid signal. We will now discuss briefly the magnitude and timescales of these effects using realistic parameters for current experiments.

From Eqs. (20) and (22), we see that the diamagnetic moment is long-lived, and the dissipation small, when $kT \ll \rho_s$. In previous work²⁸, we estimated that $\rho_s \approx 20$ mK in current experiments. This small value arises from the finite interlayer separation, and the reduced area of the sample containing superfluid in the coherence network picture. Using this estimate as well as a similar area reduction for the capacitance, we find for the attempt frequency $\omega_0 \approx 300$ MHz. Since the superfluid stiffness ρ_s is around the lowest temperatures achieved, we expect from Eq. (20) that the moments relax rapidly. Similarly, counterflow dissipation due to flux motion would be significant with $R_s^* \approx 1 - 10$ Ohm.

Activated forms similar to Eq. (22) have previously been obtained for the residual counterflow resistivity based on hopping of in-plane vortices (merons) within the

coherence network³⁰. In contrast, here we have obtained this form from the motion of phase-polarized domains, which corresponds to a large-scale collective motion of the merons. However, we expect the energy barriers for vortex motion in two dimensions to be the superfluid stiffness up to logarithmic factors, so long as the possibility of a vortex glass is excluded. Thus this form is not dependent on the precise model of vortex motion. We note that experiments on hole bilayers⁴³ see this activated behavior in the counterflow resistance with a value of 20 Ohms at 30 mK with an activated form that agrees with Eq. (19) if we use $\rho_s \approx 100$ mK. Electron bilayers⁴⁴ fit an approximately activated form with similar resistance values. A complete theory of dissipation and transport is beyond the scope of this work. Other mechanisms of dissipation will also play a role, such as the thermal excitation of vortices⁴⁵ as well as fermionic quasiparticles with an energy gap of the order of ρ_s . It suffices to point out that the contribution from flux motion is not negligible in current samples. However the activated form of Eq. (22) suggests that a modest increase in ρ_s , achievable by reducing the interlayer separation, would allow the study of the nearly dissipationless behavior of the flux-creep regime.

We now turn to the feasibility of measuring the diamagnetic response of a bilayer at low temperatures. To do this, we compare the maximum moment $M_{\parallel,\max}$ [Eq. (16)] with the scale of the perpendicular moment, $M_{\perp} = L_x L_y e \omega_c / 2$, for an electron gas in the integer quantum Hall regime with cyclotron energy $\hbar \omega_c \approx 50$ K in this system. Using our previous estimates $\rho_s \approx 20$ mK, and $L_d \approx 100 \mu\text{m}$, we obtain $M_{\parallel,\max}/M_{\perp} = (\rho_s/2\hbar\omega_c)(L_x d/L_d^2) \sim L_x/(2000 \text{ m})$ when $d = 28$ nm. This smallness of the effect, in comparison to the conventional magnetic moment, makes this very challenging to measure using torque magnetometry. This can also be inferred by noting that in our theory the critical currents in tunneling experiments are the maximum diamagnetic currents, and the former are experimentally in the nanoampere range.

However, we can exploit our understanding of the disordered isolated bilayer to consider how this diamagnetic response can be increased. In particular, we note that $M_{\parallel,\max}$ per unit volume increases with L_x and with the number of polarized domains in the sample. Note that the interlayer tunneling can be increased by many orders of magnitude compared with the current samples by reducing the tunnel barrier. Increasing the tunneling strength reduces the domain size L_d . Also, the narrower barriers possible with stronger tunneling allow a larger ρ_s . Our approach holds up to the point where the domain size L_d reaches the disorder lengthscale, $\xi \sim 100$ nm, and the maximum field B_c just reaches the depinning field B_{c2} . At this point, we obtain a significant magnetic moment $M_{\parallel,\max}/M_{\perp} \gtrsim L_x/(1 \text{ mm})$. Thus the diamagnetism of the exciton superfluid should be evident in samples with strong interlayer tunneling.

Although in the weak-tunneling samples the moments

are small, the pinning and dynamics of the in-plane flux can still be probed in transport experiments. One consequence of the pinning picture is that the critical current in a tunneling experiment should not be affected by in-plane fields smaller than B_{c2} , in contrast to the clean limit where the critical current is suppressed at fields³⁷ $B_0 < B_{c2}$. This is because in the pinning picture it is the gradients of the in-plane flux density which drive the flux through the disorder, and while the injected currents in the tunneling geometry impose such gradients, a uniform in-plane field does not. It would also be possible to study the dynamics of the in-plane flux in tunneling experiments. An interlayer voltage at one end of the sample introduces in-plane flux at a given rate, and measuring the interlayer voltages and currents reveals the subsequent motion⁴² of this flux. The logarithmic relaxation of the flux-creep regime can lead to hysteresis, which is seen in tunneling experiments¹⁹.

An interesting extension of our work would be to consider samples in the Corbino disk geometry. In such a geometry, a radial magnetic field could induce circulating counterflow supercurrents, similar to the induction of linear counterflow supercurrents by an in-plane field in the open geometry of Fig. 1. In the open geometry, tunneling is necessary to close the current loop, which we have seen gives rise to a maximum magnetic moment at the field B_c . In a Corbino disk, tunneling is not needed to close a circulating current loop, so there may be no saturation effect at B_c and the full magnetic response may persist up to B_{c2} . However, there will still be radial variations in the densities of applied flux and diamagnetic current, and maintaining the diamagnetic current loop requires that these variations are pinned. Thus it seems likely that, even in this geometry, there is a maximum magnetic moment determined by the sample dimensions and a pinning length. The relevant pinning length, however, may be determined by parameters other than the tunneling strength.

VI. CONCLUSIONS

In summary, we have considered the diamagnetic response of a bilayer exciton superfluid to an in-plane magnetic field, in the presence of in-plane vortices nucleated by charge disorder. We argue that at low temperatures, changes in the in-plane magnetic field induce circulating diamagnetic currents and hence persistent diamagnetic moments. The maximum moments which can be induced are determined by the pinning of the in-plane flux by the disorder, which involves a characteristic lengthscale related to the tunneling. At finite temperatures, thermal motion of the in-plane flux will lead to transport resistivities and cause the diamagnetic moments to decay. In current samples, we find that the maximum moments are small, but samples with stronger tunneling could allow persistent exciton supercurrents to be probed by torque magnetometry. Such experiments would be analogous to the torsional oscillator experiments that are the definitive measure of superfluid fraction in helium.

Finally, we note that very strong tunneling, or very large stiffness, may even be able to prevent the disorder nucleating vortices³¹, recovering the clean limit in which the magnetic response is also expected to be measurable²⁴. In this case the phase diagram of the bilayer would then closely parallel that of a type-II superconductor, with both a mixed state (as described here) and a clean state, experimentally distinguishable by the presence of hysteresis.

ACKNOWLEDGMENTS

We acknowledge support from Science Foundation Ireland (SFI/09/SIRG/I1592) (PRE) and EPSRC EP/F032773/1 (NRC), and we thank J. P. Eisenstein for helpful discussions.

-
- ¹ A. J. Leggett, Rev. Mod. Phys. **71**, S318 (1999).
- ² J. Blatt, K. Böer, and W. Brandt, Phys. Rev. **126**, 1691 (1962).
- ³ W. Kohn and D. Sherrington, Rev. Mod. Phys. **42**, 1 (1970).
- ⁴ E. Hanamura and H. Haug, Solid State Commun. **15**, 1567 (1974).
- ⁵ Y. E. Lozovik and V. I. Yudson, JETP Lett. **22**, 274 (1975).
- ⁶ A. V. Balatsky, Y. N. Joglekar, and P. B. Littlewood, Phys. Rev. Lett. **93**, 266801 (2004).
- ⁷ J.-J. Su and A. H. MacDonald, Nature Phys. **4**, 799 (2008).
- ⁸ Y. M. Bunkov and G. E. Volovik, J. Phys. Condens. Matter **22**, 164210 (2010).
- ⁹ M. Wouters and I. Carusotto, Phys. Rev. Lett. **105**, 020602 (2010).
- ¹⁰ J. P. Eisenstein and A. H. MacDonald, Nature **432**, 691 (2004).
- ¹¹ H. A. Fertig, Phys. Rev. B **40**, 1087 (1989).
- ¹² X. G. Wen and A. Zee, Phys. Rev. B **47**, 2265 (1993).
- ¹³ Z. F. Ezawa and A. Iwazaki, Phys. Rev. B **48**, 15189 (1993).
- ¹⁴ S. Q. Murphy, J. P. Eisenstein, G. S. Boebinger, L. N. Pfeiffer, and K. W. West, Phys. Rev. Lett. **72**, 728 (1994).
- ¹⁵ T. S. Lay, Y. W. Suen, H. C. Manoharan, X. Ying, M. B. Santos, and M. Shayegan, Phys. Rev. B **50**, 17725 (1994).
- ¹⁶ I. B. Spielman, J. P. Eisenstein, L. N. Pfeiffer, and K. W. West, Phys. Rev. Lett. **84**, 5808 (2000).
- ¹⁷ A. D. K. Finck, A. R. Champagne, J. P. Eisenstein, L. N. Pfeiffer, and K. W. West, Phys. Rev. B **78**, 075302 (2008).
- ¹⁸ Y. Yoon, L. Tiemann, S. Schmult, W. Dietsche, K. von Klitzing, and W. Wegscheider, Phys. Rev. Lett. **104**, 116802 (2010).
- ¹⁹ L. Tiemann, Y. Yoon, W. Dietsche, K. von Klitzing, and W. Wegscheider, Phys. Rev. B **80**, 165120 (2009).

- ²⁰ L. Tiemann, W. Dietsche, M. Hauser, and K. von Klitzing, New J. Phys. **10**, 045018 (2008).
- ²¹ D. W. Snoke, Adv. Condens. Matter Phys. **2011**, 938609 (2011).
- ²² J.-J. Su and A. H. MacDonald, Phys. Rev. B **81**, 184523 (2010).
- ²³ D. A. Pesin and A. H. MacDonald, Phys. Rev. B **84**, 075308 (2011).
- ²⁴ C. B. Hanna, A. H. MacDonald, and S. M. Girvin, Phys. Rev. B **63**, 125305 (2001).
- ²⁵ K. Yang, K. Moon, L. Zheng, A. H. MacDonald, S. M. Girvin, D. Yoshioka, and S.-C. Zhang, Phys. Rev. Lett. **72**, 732 (1994).
- ²⁶ S. I. Shevchenko, Phys. Rev. B **56**, 10355 (1997).
- ²⁷ D. K. K. Lee, P. R. Eastham, and N. R. Cooper, Adv. Condens. Matter Phys. **2011**, 792125 (2011).
- ²⁸ P. R. Eastham, N. R. Cooper, and D. K. K. Lee, Phys. Rev. Lett. **105**, 236805 (2010).
- ²⁹ M. M. Fogler and F. Wilczek, Phys. Rev. Lett. **86**, 1833 (2001).
- ³⁰ H. A. Fertig and G. Murthy, Phys. Rev. Lett. **95**, 156802 (2005).
- ³¹ P. R. Eastham, N. R. Cooper, and D. K. K. Lee, Phys. Rev. B **80**, 045302 (2009).
- ³² A. Stern, S. M. Girvin, A. H. MacDonald, and N. Ma, Phys. Rev. Lett. **86**, 1829 (2001).
- ³³ L. Balents and L. Radzihovsky, Phys. Rev. Lett. **86**, 1825 (2001).
- ³⁴ P. W. Anderson and Y. B. Kim, Rev. Mod. Phys. **36**, 39 (1964).
- ³⁵ L. Rademaker, J. Zaanen, and H. Hilgenkamp, Phys. Rev. B **83**, 012504 (2011).
- ³⁶ P. Bak, Reports on Progress in Physics **45**, 587 (1982).
- ³⁷ D. V. Fil, Phys. Rev. B **82**, 193303 (2010).
- ³⁸ N. Read, Phys. Rev. B **52**, 1926 (1995).
- ³⁹ M. Tinkham, *Introduction to Superconductivity* (McGraw-Hill, Inc., New York, 1996), 2nd ed.
- ⁴⁰ D. A. Huse, Phys. Rev. B **72**, 064514 (2005).
- ⁴¹ T. Nattermann and S. Scheidl, Adv. Phys. **49**, 607 (2000).
- ⁴² A. Gurevich and H. Küpfer, Phys. Rev. B **48**, 6477 (1993).
- ⁴³ E. Tutuc, M. Shayegan, and D. A. Huse, Phys. Rev. Lett. **93**, 036802 (2004).
- ⁴⁴ M. Kellogg, J. P. Eisenstein, L. N. Pfeiffer, and K. W. West, Phys. Rev. Lett. **93**, 036801 (2004).
- ⁴⁵ T. Hyart and B. Rosenow, Phys. Rev. B **83**, 155315 (2011).